Maturing ECRF Technology for Plasma Control

R.W. Callis,[1] W.P. Cary,[1] S. Chu,[2] J.L. Doane,[1] R.A. Ellis,[3] K. Felch,[2] Y.A. Gorelov,[1] H.J. Grunloh,[1] J. Hosea,[3] K. Kajiwara,[1] J. Lohr,[1] T.C. Luce,[1] J.J. Peavy,[1] R.I Pinsker,[1] D. Ponce,[1] R. Prater,[1] M. Shapiro,[4] R.J. Temkin,[4] J.F. Tooker[1]

[1]General Atomics, P.O. Box 85608, San Diego, CA 92186-5608 USA
e-mail: callis@fusion.gat.com
[2]Communications and Power Industries, 811 Hansen Way, Palo Alto, CA 94304 USA
[3]Princeton Plasma Physics Laboratory, P.O. Box 451, Princeton, NJ 08543-0451 USA
[4]Plasma Science and Fusion Center, MIT, 167 Albany St. Cambridge, MA 02139 USA

Abstract. The availability of high power, (~1 MW) long pulse length (effectively cw), high frequency, (>100 GHz) gyrotrons has opened the opportunity for enhanced scientific results on magnetic confinement devices for fusion research worldwide. This has led to successful experiments on electron cyclotron heating, electron cyclotron current drive, non-inductive tokamak operation, tokamak energy transport, suppression of instabilities and advanced profile control leading to enhanced performance. The key development in the gyrotron community that has led to the realization of high power long pulse gyrotrons is the availability of edge cooled synthetic diamond gyrotron output windows, which have low loss and excellent thermal and mechanical properties. In addition to the emergence of reliable high power gyrotrons, ancillary equipment for efficient microwave transmission over distances of hundreds of meters, polarization control, diagnostics, and flexible launch geometry have all been developed and proven in regular service.

1. Introduction

Since present day research devices and, more importantly, future reactor-like devices need multi-megawatt electron cyclotron heating (ECH) systems, it has been a long time goal of microwave tube manufacturers to develop a 100+ GHz tube that can operate at 1 MW continuously, with a reasonably high efficiency. It appears that the internal mode-converter gyrotrons [1,2] with a CVD diamond window meet this objective. Thermal stresses developed in the output window have been the major technical roadblock to achieving a reliable 1 MW, cw gyrotron. Sapphire and boron nitride have been successfully used in MW class gyrotrons with pulse length as high as 2 s. But it has only been with the development of low-loss, large, CVD diamond disks [3] that true 1 MW, cw gyrotrons have become available.

To transport the rf energy from the gyrotron to the tokamak, the DIII–D system uses an evacuated low-loss corrugated transmission line, up to 100 m in length with up to 14 90° mitre bends. The transmission efficiency of this system is about 80%. The transmission lines also incorporate customized diagnostic devices that are used to characterize the rf beam. To facilitate all experiments that require use of ECH, launchers, located on the outer upper ports of the DIII–D vacuum vessel, must have the ability to scan the rf beam both poloidally and toroidally in order to locate the beam on- and off-axis, and to support both co- and counter-current drive.

2. ECH System and Hardware Development

2.1. Overview

The 110 GHz ECH system for the DIII–D tokamak consists of six assemblies. Each assembly comprises a gyrotron, a gyrotron superconducting magnet, a gyrotron/magnet supporting tank, a low loss transmission line, a launcher and associated controls. Three of the gyrotrons were manufactured by GYCOM and have a nominal output of 800 kW for 2 s, with the pulse length limit resulting from the peak temperature allowed on the boron nitride output window. The three long-pulse gyrotrons are manufactured by Communication and Power Industries (CPI) and have a nominal rating of 1 MW, for 10 s. All internal-elements of these gyrotrons are expected to be in thermal equilibrium at 10 s; therefore a cw rating is possible for these units.

2.2. Long Pulse Gyrotron

The three long pulse 110 GHz gyrotrons used in the DIII–D ECH system are an internal-mode-converter design (shown in Fig 1) with a Gaussian output rf beam. Each gyrotron has a hollow, annular electron beam produced by a magnetron-injection-type electron gun in a diode geometry. The hollow electron beam is compressed by the gyrotron superconducting magnet and excites the $TEM_{22,6,1}$ cavity eigenmode. The rf power generated in the cavity has a complex structure that does not lend itself to low-loss propagation. To achieve the desired low-loss propagation, the rf wave must be formed into a Gaussian-like rf beam, which is achieved using a dimpled-wall mode-converter launcher [4]. A series of relay mirrors is used to direct the rf beam out of the gyrotron. These mirrors can also be used to make final correction to the phase and profile of the beam, such that at the output window the beam has good Gaussian qualities.

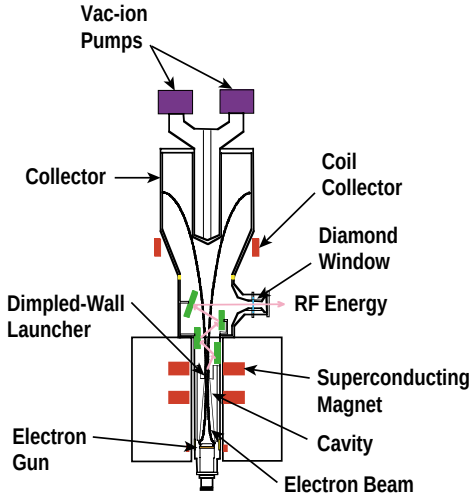

Fig. 1. Schematic diagram of a CPI 110 GHz, 1 MW gyrotron with CVD diamond output window.

2.3. CVD Diamond Window

Previous gyrotron output window material had either relatively high loss, 4% for boron nitride, or poor thermal conductivity (sapphire), that limited the pulse length at 1 MW to a few seconds at best. These windows also required spreading the rf beam in a non-Gaussian profile, which needed to be converted back to Gaussian externally to the gyrotron, resulting in a loss of 10% of the rf power at minimum. CVD diamond also has the beneficial characteristic of a high thermal conductivity of 2000 W/m°K, about four times that of copper, which allows simple edge cooling to extract all the energy absorbed (~0.2%) as the rf beam passes through. Figure 2 shows that the window comes into thermal equilibrium in about 3 s.

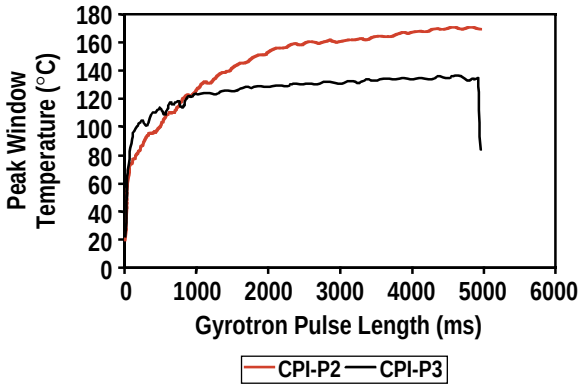

Fig. 2. Peak window temperature for a ~1 MW, 5 s pulse from CPI-P2 and CPI-P3. Cooling water temperature was 22°C. Note the higher window temperature for CPI-P2, which may have a graphite film on its inside surface.

2.4. Transmission Line System

All gyrotrons are connected to the tokamak by a low-loss windowless, evacuated transmission line using 31.75 mm diameter circular corrugated waveguide for propagation in the HE_{11} mode (see Fig. 3). Transmission efficiencies of the waveguide lines have been measured directly, indicating 20% loss in about 100 m line length with eleven miter bends. Each waveguide system incorporates a two-mirror launcher in the tokamak, which can steer the rf beam poloidally from the center to the outer edge of the plasma. The launcher system now installed can also scan ~±20° in toroidal direction. A poloidal scan across the tokamak upper half plane takes about 2 s, a rate suitable for tracking target features in the plasma. Precise control of the location of the driven current made possible by the flexibility of these launchers can in turn lead to control of the current density profile.

Rapid calorimetric response has been achieved with mode-conversion dummy loads. Loads have been fabricated in dispersion-strengthened copper with internal nickel plating to increase the absorption and with external corrugations to improve the water cooling. When 1 MW was incident in several 5 s pulses, over 800 kW was absorbed at 110 GHz in a load 1.8 m long.

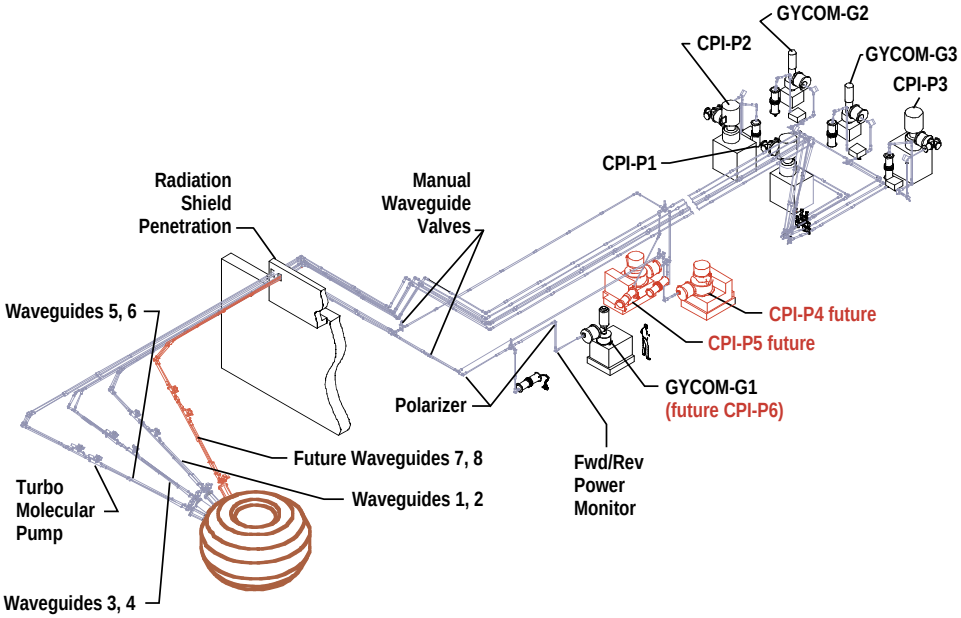

Fig. 3. Layout of the DIII–D ECH system including the future transmission lines and gyrotrons as well as key transmission line components.

3. Experimental Results

3.1. Current Drive

ECH with its precisely localized heat and current drive capabilities is an excellent tool to support the exploration of advanced tokamak physics [5]. ECH current drive efficiency is higher at the center of the plasma where the temperature peaks. There was a concern that the efficiency of the off-axis current drive would be unacceptably low where it is needed for AT plasma and stability control. The decreased efficiency is caused by trapping effects, which push electrons into trapped orbits in which they cannot contribute to current drive. However, initial off-axis experiments at the megawatt level and theoretical modeling, do not show the dramatic drop off in current drive, as shown in the low β case in Fig. 4. The key to this phenomenon is that as the local electron beta is increased, the resonant electrons are moved away from the trapping boundary in phase space and more electrons participate in driving current. Electron cyclotron driven currents of 120 kA have been measured on DIII–D with excellent agreement with the Fokker-Planck modeling code CQL3D.

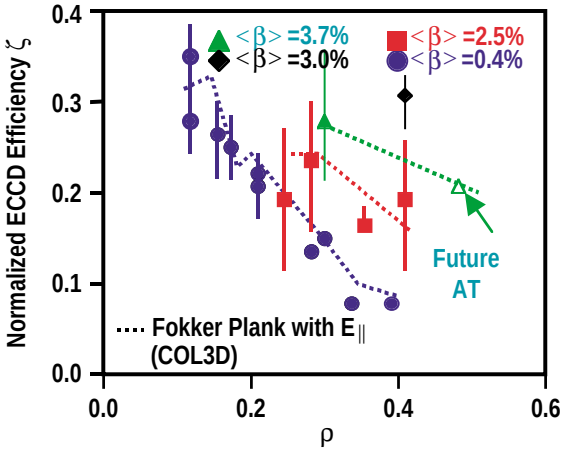

Fig. 4. Experimental ECCD efficiency as a function of the normalized radius of deposition for <β> = 0.4% (circles), <β> = 2.5% (squares), <β> = 3.0% (diamonds), and <β> = 3.7% (triangles). The theoretical ECCD efficiency is also shown (dashed lines).

3.2. NTM Stabilization

The neoclassical tearing mode (NTM) is generated when the local electron pressure gradient is reduced and cannot support the gradient-driven bootstrap current. This usually occurs at low-order-rational surfaces (e.g. q = 3/2, 2/1), with the 3/2 mode being the most dominant [6]. ECCD experiments on DIII–D have demonstrated a complete suppression of both the 3/2 and 2/1 NTM, which resulted in subsequent plasma performance exceeding the initial level, as long as the ECH power was on. Suppression of the 2/1 mode is clearly shown in Fig. 5. NTM suppression is very sensitive to the placement of the rf beam, and a radial shift of the 8 cm

diameter beam by as little as 2 cm loses the suppression effect [7].

3.3. Current Profile Control

The DIII–D AT program has demonstrated the feasibility of sustaining conditions that combine high fusion power density ($\beta > 4\%$) and high bootstrap current fraction (~65%) for ~4 τ_E. The duration of the high performance conditions is limited only by evolution of the current profile. Modeling indicates that with density control consistent with that achieved experimentally, off-axis electron-cyclotron current drive should be able to maintain a favorable current density profile for several seconds. Experiments have shown that the electron current density $j_{||}(\rho)$ and the q profile can be substantially changed by use of ECCD, as shown in Fig. 6.

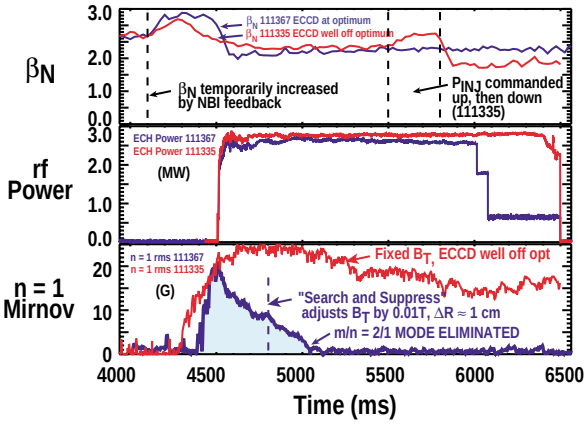

Fig. 5. Approximately 2.3 MW of ECCD is used to suppress a n/m=2/1 NTM in discharge #111367. Compared to a similar discharge, #111335, in which the resonance is well off optimum, DR ≈ 10 cm.

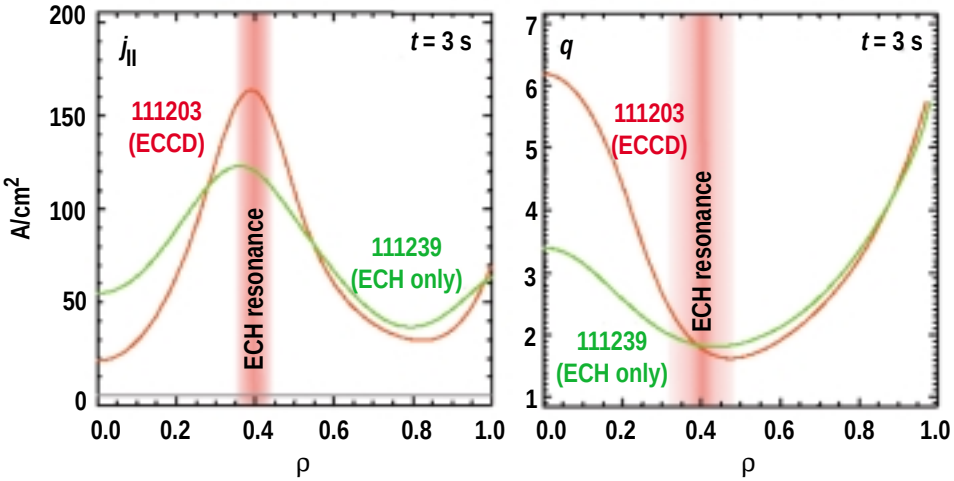

Fig. 6. Modification of the electron current density profile $j_{||}(\rho)$, and the q profile by ECH and ECCD, both injected at ρ=0.4.

Acknowledgment

Work supported by U.S. Department of Energy under Contracts DE-AC03-99ER54463, DE-AC02-76CH03073, and DE-FC02-93ER54186.

References

[1] M.V. Agapova, *et.al.*, Proc. 20th Int. Conf. on Infrared and Millimeter Waves, Ed. R. Temkin, Cocoa Beach, Florida, 205, 1995.
[2] K. Felch, *et al.*, Proc 22nd Int. Conf on Infrared and Millimeter Waves, Ed. T.J. Parker and S.R.P. Smith, Colchester, England, 367–368, (1998).
[3] K. Takahashi, *et al.*, Rev. Sci. Instruments, **71**, 4139 (2000).
[4] G.G. Denisov, *et al.*, Int J. Electronics, **72**, 1079 (1992).
[5] C.C. Petty, *et al*. Proc. 14th Topical Conference on Radio Frequency Power in Plasmas, Oxnard, California, 275 (2001).
[6] B. Lloyd, Proc. 14th Topical Conference on Radio Frequency Power in Plasmas, Oxnard, California, 33 (2001)
[7] T.C. Luce, *et al.*, 14th Topical Conference on Radio Frequency Power in Plasmas, Oxnard, California, 306 (2001).